Prosthetic Legs Output Feedback Control via Variable High Gain Observer

Alessandro J. Peixoto, Ignácio de A. M. Ricart and Matheus Ferreira dos Reis

***Abstract*— This paper address the state estimation and control of a robot/prosthesis control system with four joints: vertical hip displacement, thigh, knee and ankle angles. The motivation was inspired by several drawbacks regarding the usage of load cells and/or sensors in robots and prosthetic legs to capture gait data, external forces (GRFs) and moments during walking. We propose the implementation of a high gain observer (HGO) to estimate the prosthesis joint velocities with a time-varying HGO gain synthesized from measurable signals designed to reduce the amount of noise in the control effort while keeping an acceptable tracking error transient performance. Numerical simulations analyze the robustness of the closed-loop control with respect to parametric errors and measurement noise.**

I. Introduction

Prostheses are devices that substitute the function of a missing limb either due to amputation or a congenital defect. Amputations could occur due to injuries, circulatory and vascular disease, diabetes, smoking or cancer. This means, a huge number of people that could maintain their activities of daily livings (ADLs) and have the mobility partially/completely restored through improvements in prosthesis technology.

The lower limb amputation could be at the foot, including toes or partial foot, at the ankle (ankle disarticulation), below the knee (transtibial), at the knee (knee disarticulation), above the knee (transfemoral) or at the hip (hip disarticulation). Depending on which residual limb remains, mobility could be restored by using a prosthetic foot or, in a worst case scenario, the combination of prosthetic foot/ankle, shin/pylon, prosthetic knee and a socket interfacing the residual limb with the prosthetic leg.

During the gait, hip, thigh, knee and ankle move expending the minimum metabolic energy, a behavior that resembles that of passive mechanical systems. This motivates the design os prosthesis with moving parts coupled by springs and dampers. Nevertheless, it is also important to generate net power in prosthetic joints through DC electrical motors, pneumatic or hydraulic actuators [1] [2] so that amputees could also realize tasks such as climbing stairs and walking uphill.

Because of that, passive mechanical systems could be used in prosthetics systems, such as springs and dampers with controlled levels as Endolites ankle products and Otto Empower Ankle. However, being able to generate net power in prosthetic joints through DC electrical motors, pneumatic or hydraulic actuators [1] [2] is important so that amputees could also realize tasks such as climbing stairs and walking uphill.

Commonly, the joints angles in a prosthesis are measured with high-resolution encoders, while contact forces are obtained via strain gauges and load cells. Angular velocities could be acquired through expensive tacometers or via estimation.

In general, numerical approaches for velocity are implemented via state observers or derivative filters, like lead filter. However, noise attenuation is a well known challenge in those cases. In this direction, state estimation via Extended Kalman Filter (EKF), High-gain-observer (HGO) and Sliding Mode Observer (SMO) are promising approaches. These techniques could also be used to estimate the contact forces acting on a prosthetic foot.

In contrast to [3], where an EKF is designed to estimate joint position, velocities and ground reaction forces, here an HGO based estimation approach is deployed. Time-varying HGOs have also been used to cope with the effect of measurement noise and to establish the connections with the EKF [4] [5].

Output-feedback control strategies using HGOs [6] represent an important design class, in particular, the schemes based on time-varying techniques (HGO with variable gain) [7] [8] [9] [10] [4]. In [11], [12], an output-feedback sliding-mode control design have been proposed for arbitrary relative degree uncertain systems, where the class of plants encompasses time-varying minimum phase nonlinear plants, affine in the control, transformable to a normal form and for which a norm state estimator can be implemented. The main objective in [11] was to use a dynamic observer gain in order to obtain global results without invoking global Lipschitz-like restrictions.

In the present paper, considering that a robot/prosthesis system has parametric uncertainties and angle measurement is subject to noise, a time-varying HGO design is proposed, similar to [11]. This variable gain approach is different from most of the existing techniques, where the HGO gain is updated either solving a Riccati equation [7] [13] [14] or via functions based on measurable signals and norm domination techniques [10], [13], [15] and [11].

While estimating in real-time the noise energy presented in the control effort, an adaptation law changes the observer gain to achieve a acceptable trade-off between control signal noise and tracking performance. It is important to note that, although global results are not pursued in this paper, the proposed technique is easily applicable to practical scenarios, given that bounds for the system states are known a priori.

A proportional-integral-derivative (PID) conventional control with feedback linearization is developed in order to make

a robotic prosthetic leg follow a desired walking pattern.

The proposed approach is verified in a simulation environment with a 4-link robot/prosthesis system (PRRR), with parameters extracted from [16] and motion limited to the sagittal plane. The human gait used as reference signal is obtained from [17].

II. Preliminaries

The following notations and terminology are used:

- The 2-norm (Euclidean) of a vector x and the corresponding induced norm of a matrix A are denoted by $|x|$ and $|A|$, respectively. The symbol $\lambda[A]$ denotes the spectrum of A and $\lambda_m[A] = -\max_i\{Re\{\lambda[A]\}\}$.
- The $\mathscr{L}_{\infty e}$ norm of a signal $x(t)\in\mathbb{R}^n$ is defined as $\|x_t\| := \sup_{0\leq\tau\leq t}|x(\tau)|$.
- The symbol "s" represents either the Laplace variable or the differential operator "d/dt", according to the context.
- As in [18] the output y of a linear time invariant (LTI) system with transfer function $H(s)$ and input u is given by $y = H(s)u$. Convolution operations $h(t)*u(t)$, with $h(t)$ being the impulse response from $H(s)$, will be eventually written, for simplicity, as $H(s)*u$.
- Classes of $\mathscr{K},\mathscr{K}_\infty$ functions are defined according to [19, p. 144]. ISS, OSS and IOSS mean Input-State-Stable (or Stability), Output-State-Stable (or Stability) and Input-Output-State-Stable, respectively [20].
- The symbol π denotes class-$\mathscr{KL}$ functions. Eventually, we denote by $\pi(t)$ any exponentially decreasing signal, i.e., a signal satisfying $|\pi(t)| \leq \Pi(t)$, where $\Pi(t) := Re^{-\lambda t}$, $\forall t$, for some scalars $R,\lambda > 0$.

III. System Model

The dynamics of the machine/prosthesis system composed by a 4-link rigid body robot[1] with prismatic-revolute-revolute-revolute (PRRR) configuration, following the notation in [16], is given by:

$$D(q)\ddot{q} + C(q,\dot{q})\dot{q} + B(q,\dot{q}) + P(\dot{q}) + J_e^T F_e + g(q) = F_a\,, \quad (1)$$

where q represents the vector of joints positions (q_1 represents the hip vertical displacement, q_2 is the thigh angle, q_3 is the knee angle and q_4 represents ankle angle), $D(q)$ is the inertia matrix, $C(q,\dot{q})$ is the matrix of Coriolis and centrifugal forces, $B(q,\dot{q})$ is the knee damper nonlinear matrix, J_e is the kinematic Jacobian relative to the point of application of external forces F_e, $g(q)$ is the term of gravitational forces and F_a is the torque/force produced by the actuators. The term $P(\dot{q})$ explicitly represents the Coulomb friction as in [21]. Note that, inertial and frictional effects in the actuators can be included in this model.

To establish a basis for dynamic model derivations and to verify the leg geometry during simulations, the set of reference frames used for forward kinematics problems are the same as the ones assigned in [16]. Matrices $D(q)\ddot{q}$, $C(q,\dot{q})$ and $g(q)$ are obtained using the standard Newton-Euler/Euler-Lagrange approach with the plant parameters extracted from [16].

[1] A more general framework with a n-link rigid body robot can also be considered. However, in order to keep this note close to [16], for simplicity, we have set $n = 4$.

A. A Simplified Model

In order to illustrate the observer design proposed in this note, consider a simplified version of the machine/prosthesis system (2) where no external forces are considered ($F_e \equiv 0$), the specific leg prosthesis damping matrix is disregarded ($B(q,\dot{q}) \equiv 0$) and the Coulomb friction is neglected ($P(\dot{q}) \equiv 0$). In this case, the machine/prosthesis system is described by:

$$D(q)\ddot{q} + C(q,\dot{q})\dot{q} + g(q) = F_a\,. \quad (2)$$

The system matrices $D(q), C(q,\dot{q})$ and $g(q)$ are supposed to be uncertain, but the corresponding nominal matrices $D_n(q), C_n(q,\dot{q})$ and $g_n(q)$ are assumed known. In particular, the inertia matrix $D(q)$ which is invertible, since $D(q) = D^T(q)$ is strictly positive defined.

Introducing the variables $x_1 := q \in \mathbb{R}^4$ and $x_2 := \dot{q} \in \mathbb{R}^4$, the model (2) can be rewritten in the state-space form as:

$$\begin{aligned} \dot{x}_1 &= x_2\,, && (3a)\\ \dot{x}_2 &= k_p(x,t)\,[u + d(x,t)]\,, \quad u := F_a \in \mathbb{R}^{4\times 1}\,, && (3b)\\ y &= x_1\,, && (3c) \end{aligned}$$

or, equivalently,

$$\begin{aligned} \dot{x} &= A_\rho x + B_\rho k_p(x,t)[u + d(x,t)]\,, && (4a)\\ y &= C_\rho x\,, && (4b) \end{aligned}$$

where $x^T = \left[\begin{array}{cc} x_1 & x_2 \end{array}\right]$ is the state vector, $k_p(x,t) = D(x_1)^{-1} \in \mathbb{R}^{4\times 4}$, $d(x,t) := -C(x_1,x_2)x_2 - g(x_1) \in \mathbb{R}^{4\times 1}$, $C_\rho = \left[\begin{array}{cc} I_{4\times 4} & 0_{4\times 4} \end{array}\right] \in \mathbb{R}^{4\times 8}$ and the pair (A_ρ, B_ρ) is in Brunovskys canonical controllable form and is given by:

$$A_\rho = \left[\begin{array}{cc} 0_{4\times 4} & I_{4\times 4} \\ 0_{4\times 4} & 0_{4\times 4} \end{array}\right] \in \mathbb{R}^{8\times 8}\,,$$

and

$$B_\rho = \left[\begin{array}{cc} 0_{4\times 4} & I_{4\times 4} \end{array}\right]^T \in \mathbb{R}^{8\times 4}\,.$$

For each solution of (4a) there exists a maximal time interval of definition given by $[0,t_M)$, where t_M may be finite or infinite. Thus, finite-time escape is not precluded, *a priori*.

IV. High Gain Observer with Variable Gain

The HGO [22] is given by

$$\dot{\hat{x}} = A_\rho\hat{x} + B_\rho k_p^n u + H_\mu L_o(y - C_\rho\hat{x})\,, \quad (5)$$

where k_p^n is a nominal value of the plant high frequency gain (HFG) k_p and L_o and H_μ are given by:

$$\begin{aligned} L_o &= \left[\begin{array}{cc} l_1 I_{4\times 4} & l_2 I_{4\times 4} \end{array}\right]^T \in \mathbb{R}^{8\times 4} && (6a)\\ H_\mu &:= \mathrm{diag}(\mu^{-1} I_{4\times 4},\ \mu^{-2} I_{4\times 4}) \in \mathbb{R}^{8\times 8}\,. && (6b) \end{aligned}$$

The observer gain L_o is such that $s^2 + l_1 s + l_2$ is Hurwitz. In this paper, instead of using a constant μ, we introduce a *variable* parameter $\mu = \mu_(t) \neq 0, \forall t \in [0,t_M)$, of the form

$$\mu(\omega,t) := \frac{\bar{\mu}}{1 + \psi_\mu(\omega,t)}\,, \quad (7)$$

where ψ_μ, named **adapting function**, is a non-negative function continuous in its arguments and ω is an available signal, both to be designed later on. The parameter $\bar{\mu}>0$ is a design constant. For each system trajectory, μ is absolutely continuous and $\mu \leq \bar{\mu}$. Note that μ is bounded for t in any finite sub-interval of $[0,t_M)$. Therefore,

$$\mu(\omega,t) \in [\underline{\mu},\bar{\mu}], \quad \forall t \in [t_*,t_M), \tag{8}$$

for some $t_* \in [0,t_M)$ and $\underline{\mu} \in (0,\bar{\mu})$.

A. High Gain Observer Error Dynamics

The transformation [6]

$$\zeta := T_\mu \tilde{x}, \quad T_\mu := [\mu^2 H_\mu]^{-1} \in \mathbb{R}^{8\times 8}, \quad \tilde{x} := x - \hat{x}, \tag{9}$$

is fundamental to represent the $\tilde{x}$-dynamics in convenient coordinates allowing us to show that $\tilde{x}$ is arbitrarily small, *modulo* exponentially decaying term. First, note that:

$$(i)\ T_\mu(A_\rho - H_\mu L_o C_\rho)T_\mu^{-1} = \frac{1}{\mu}A_o, \quad (ii)\ T_\mu B_\rho = B_\rho,$$

$$\text{and} \quad (iii)\ \dot{T}_\mu T_\mu^{-1} = \frac{\dot{\mu}}{\mu}\Delta,$$

where $A_o := A_\rho - L_o C_\rho$ and $\Delta := \mathrm{diag}(-I_{4\times 4},\ 0_{4\times 4}) \in \mathbb{R}^{8\times 8}$. Then, subtracting (5) from (4a) and applying the above relationships (i), (ii) and (iii), the dynamics of $\tilde{x}$ in the new coordinates ζ (9) is given by:

$$\mu\dot{\zeta} = [A_o + \dot{\mu}(t)\Delta]\zeta + B_\rho[\mu\nu], \tag{10}$$

where

$$\nu := (k_p - k_p^n)u + k_p d, \tag{11}$$

and

$$\dot{\mu}(t) = -\frac{\mu^2}{\bar{\mu}}\left[\frac{\partial \psi_\mu}{\partial \omega}\dot{\omega} + \frac{\partial \psi_\mu}{\partial t}\right]. \tag{12}$$

The HGO gain ($H_\mu L_o$) is inversely proportional to the small parameter μ, allowed to be time-varying. Our task is to establish properties for the adapting function $\psi_\mu(\omega,t)$ in (7) so that $\mu|\nu|$ and $|\dot{\mu}|$ are arbitrarily small, at least after a finite time interval. In fact, we design ψ_μ so that the following inequalities hold

$$|\dot{\mu}(t)|,\ \mu|\nu| \leq \mathscr{O}(\bar{\mu}), \quad \forall t \in [t_\mu,t_M). \tag{13}$$

for some finite $t_\mu \in [0,t_M)$. Consequently, $\dot{\mu}$ does not *ultimately* affect the stability of A_o in (10) and ζ can be made arbitrarily small, *modulo* an exponentially decaying term, by applying a time scale changing in (10). In addition, since $\tilde{x} = T_\mu^{-1}\zeta$ and $\|T_\mu^{-1}\|$ is of order $\mathscr{O}(1)$, then one can conclude that $\tilde{x}$ can also be made arbitrarily small, *modulo* an exponentially decaying term.

It is clear that inequalities in (13) depend on the choice of the control signal u in (11), the disturbance and the signal ω.

B. The Adapting Function ψ_μ

The adapting function $\psi_\mu(\omega,t)$ used in the time-varying parameter

$$\mu(\omega,t) := \frac{\bar{\mu}}{1+\psi_\mu(\omega,t)}, \tag{14}$$

defined in (7), can assume different forms depending on the choice of the signal ω and the available information about the plant.

As an example, consider the following cases:

1) **From a theoretical point of view**: the adapting function ψ_μ can be chosen in order to allow global/semi-global stability (or only convergence) properties for the closed-loop control system.
   a) **Norm Observability**: The plant (4a)–(4b) admits a norm observer which provides an upper bound for the plant state norm by using only available signals: plant input (u) and plant output (y). In this case, global or semi-global results could be obtained when, for example, a sliding mode based control is employed, as in [11].
   More precisely, a norm observer for system (4a)–(4b) is a m-order dynamic system of the form:

$$\tau_1\dot{\omega}_1 = -\omega_1 + u, \tag{15}$$

$$\tau_2\dot{\omega}_2 = \gamma_o(\omega_2) + \tau_2\varphi_o(\omega_1,y,t), \tag{16}$$

   with states $\omega_1 \in \mathbb{R}$, $\omega_2 \in \mathbb{R}^{m-1}$ and positive constants τ_1,τ_2 such that for $t \in [0,t_M)$: (i) if $|\varphi_o|$ is uniformly bounded by a constant $c_o>0$, then $|\omega_2|$ can escape at most exponentially and there exists $\tau_2^*(c_o)$ such that the ω_2-dynamics is BIBS (Bounded-Input-Bounded-State) stable w.r.t. φ_o for $\tau_2 \leq \tau_2^*$; (ii) for each $x(0),\omega_1(0),\omega_2(0)$, there exists $\bar{\varphi}_o$ such that

$$|x(t)| \leq \bar{\varphi}_o(\omega(t),t) + \pi_o(t), \quad \omega := [\omega_1\ \ \omega_2^T\ \ y]^T, \tag{17}$$

   where $\pi_o := \beta_o(|\omega_1(0)|+|\omega_2(0)|+|x(0)|)e^{-\lambda_o t}$ with some $\beta_o \in \mathscr{K}_\infty$ and positive constant λ_o.
   b) **Global Stability Properties**: when the class of plants are such that a norm observer can be implemented, then **global** results can be achieved via OFSM control, as in [11]. This is the case when, for example, the Coriolis term can be neglected ($C(x_1,x_2)x_2 \equiv 0$).
   c) **Semi-Global Stability Properties**: it is not a restrictive assumption consider the existence of a class $\mathscr{K}_\infty$ function $\Psi(\cdot)$ and an positive constant k_ψ such that

$$\|d(x,t)\| \leq \Psi(\|x\|) + k_\psi,$$

   $\forall x$ and $\forall t$. In other words, the disturbance can always be norm bounded afinelly in the state norm, when it is norm bounded in the second argument. Thus, given $R>0$ and $0<R_0<R$, then for some $t^* \in (0,t_M)$ and $\|x(0)\|<R_0$ one has $\|x(t)\|<R$ for $t \in [0,t^*)$. Assume $t \in [0,t^*)$. Since the nonlinear terms in the robot dynamic equation are usually assumed sufficiently smooth and locally Lipschitz in its arguments, then $\Psi(\cdot)$ can be chosen locally Lipschitz in it argument.

In addition, while $t \in [0, t^*)$, the state x is bounded by the arbitrary constant R. Thus, one has that the following upper bound holds $\Psi(\|x\|) \leq \kappa(R)\|x\|$, where $\kappa(\cdot)$ being of class $\mathscr{K}$. For a given R, $\kappa(R)$ is a positive constant which increases as $R \to +\infty$, but is not necessarily unbounded. By noting that R depends on the initial condition (due to R_0), then only **semi-global** stability properties follows. In fact, this semi-global result can be obtained via a particular case of the OFSM control given in [11]. This is the case when, for example, the Coriolis term can not be neglected ($C(x_1, x_2)x_2 \neq 0$).

2) **From a practical point of view**: the adapting function ψ_μ can be chosen in order to allow local stability (or only convergence) properties for the closed-loop control system. Moreover, one can select a time-varying adapting function ψ_μ to assure an acceptable level of noise in the control signal while keeping a good transient for the output tracking error.

   a) **The system states can be assumed bounded**: The plant state, in particular the unavailable state x_2, is uniformly bounded. Such assumption of the state boundedness is true, for example, when (4a) is BIBS stable, and the control input is bounded. Moreover, by considering that the acceleration ($\dot{x}_2$) in the mechanical system is bounded by a known constant, then a constant upper bound for the velocity x_2 can be found by using the "dirty derivative":

$$\eta := \frac{\tau}{\tau s + 1} y. \tag{18}$$

   Indeed, by noting that

$$x_2 = \eta + \frac{\tau}{\tau s + 1} \dot{x}_2, \tag{19}$$

   one can obtain the following norm bound

$$|x_2| \leq |\eta| + \mathscr{O}(\tau)\,|\dot{x}_2|. \tag{20}$$

   In this case, we can use this rough estimate for $\dot{x}_2$ and less conservative estimates for the terms depending on y, so that ω can be implemented.

   b) **Signal-to-Noise Ratio in $|u|$ $\times$ Tracking Error Norm**: By using some measurement of the amount of noise in the control signal, for example, the Signal-to-Noise Ratio (SNR), the adapting function can be implemented as a function of the SNR and the tracking error, so that μ increases when the SNR in the control effort increases and μ decreases when the tracking error norm increases. This can be accomplished, for example, by defining a cost function depending on the control signal-to-noise ratio and the output tracking error, so that the time-varying μ reaches an optimum value.

C. One Particular Design for ψ_μ

In this paper, we are focused in the following particular choice for time varying HGO gain $\mu(t)$ where noise energy in the control signal and tracking error are taken into account:

$$\mu(\omega, t) := \frac{\alpha \mathscr{N}\{u\}}{1 + \beta|e|} = \frac{\bar{\mu}}{1 + \psi_\mu(\omega, t)}, \tag{21}$$

where α, β are positive design constants, $\mathscr{N}\{u\} > 0$ is the noise energy presented in the control effort $u(t)$ and e is the tracking error. Note that, this choice fits the general format (7) with $\psi_\mu(\omega, t) = [(1 + \beta|e|)\bar{\mu} - \alpha\mathscr{N}\{u\}]/(\alpha\mathscr{N}\{u\})$ and $\bar{\mu}$ small enough to assure that $\psi_\mu(\omega, t) > 0$.

The noise energy is obtained by filtering the norm of the difference between the upper U^+ and lower U^- envelopes of the control signal u which is contaminated by noise. The noise energy $\mathscr{N}\{u\}$ is defined as:

$$\mathscr{N}\{u(t)\} := \frac{1}{\tau_n s + 1} \left| U^+(t) - U^-(t) \right|,$$

where $\tau_n > 0$ is a design constant. Several on-line methodologies for estimation of noise energy in a available signal (Signal-to-Noise Ratio) can be found in the literature. A fair comparison is left for a future work.

Note that, in this case, the time derivative $\frac{d\mathscr{N}\{u(t)\}}{dt}$ can be norm bounded if the noise energy is norm bounded, which is reasonable to assume. Therefore, one can verify that (13) holds following the a similar approach as the one described in [11].

D. Norm Bounds for the HGO Estimation Error

The following lemma can be stated.

Lemma 1. *Consider the HGO error dynamics (10). Then, if the HGO time varying parameter $\mu(t)$ in (7) is designed to satisfy (13) during the interval $t \in [t_\mu, t_M)$, then the observer error norm $|\tilde{x}(t)|$ is bounded by a constant of order $\mathscr{O}(\bar{\mu})$,* modulo *an exponentially decaying term depending on the HGO initial condition.*

Proof: Consider the ζ-dynamics (10) and the storage $V = \zeta^T P \zeta$, where $P = P^T > 0$ is the solution of $A_o^T P + P A_o = -I$. Then, the time derivative of V along the solutions of (10) satisfies $\mu\dot{V} = -|\zeta|^2 + (\dot{\mu})[2\zeta^T P \Delta\zeta] + (\mu\nu)[2\zeta^T P B_\rho]$. Now, designing μ to satisfy (13), the following inequality is valid $\forall t \in [t_\mu, t_M)$: $\mu\dot{V} \leq -|\zeta|^2 + \mathscr{O}(\bar{\mu})k_1|\zeta|^2 + \mathscr{O}(\bar{\mu})k_2|\zeta|$, where $k_1 := 2|P||\Delta|$ and $k_2 := 2|P||B_\rho|$. Moreover, since $ab < a^2 + b^2$, for any positive real numbers a, b, then

$$\mu\dot{V} \leq -[1 - \mathscr{O}(\bar{\mu})k_1 - \mathscr{O}(\bar{\mu})]|\zeta|^2 + \mathscr{O}(\bar{\mu}),$$

from which one can conclude that $\mu\dot{V} \leq -\lambda_1 V + \mathscr{O}(\bar{\mu})$, with an appropriate constant $\lambda_1 > 0$. Now, either $V \leq 2\mathscr{O}(\bar{\mu})/\lambda_1$ or $\mu\dot{V} \leq -\lambda_1 V/2$. Consider the later case. Since $\mu < \bar{\mu}$, then one has $\dot{V} \leq -\lambda_1 V/(2\bar{\mu})$. Hence, one can conclude that

$$|\zeta|, |\tilde{x}| \leq \beta_2(|\zeta(0)|)e^{-\lambda_2 t} + \mathscr{O}(\bar{\mu}),$$

$\forall t \in [t_\mu, t_M)$, with an appropriate constant $\lambda_2 > 0$ and some $\beta_2 \in \mathscr{K}_\infty$. In the last inequality, the norm bound for $\tilde{x}$ was obtained by reminding that $\tilde{x} = T_\mu^{-1}\zeta$, by definition, which implies $|\tilde{x}| \leq |\zeta|$, since $|T_\mu^{-1}| \leq 1$ for $\mu < 1$. ∎

V. Problem Formulation and Control Schemes Stability Properties

The *control objective* is to reduce the tracking error

$$e(t) := y_d - y, \tag{22}$$

where the desired trajectory y_d is ideally a set of joint angles acquired for human gait analysis [17]. A second-order model reference linear filterhas been designed so that the reference signal is actually a filtered version of human gait desired angles. This allows us to obtain directly the time-varying derivatives $\dot{y}_d$ and $\ddot{y}_d$ from the state vector representation of the model reference filter.

In order to focus on the behaviour of the HGO with time varying gain, a simple PID controller with feedforward is employed in this note. So, only local stability properties are assured in presence of uncertainties in the plant parameters and in the HGO estimates. Global/semi-global stability properties can be obtained by using the OFSM controller previously developed in [11].

By recalling that we consider $D_n(y) = D(y)$ to simplify the paper presentation, the control signal is given by

$$u(t) := D(y)u_v + C_n(y,\hat{x}_2)\hat{x}_2 + g_n(y), \tag{23}$$

$$u_v(t) := \ddot{y}_d + K_p e(t) + \underbrace{K_d(\dot{y}_d - \hat{x}_2)}_{\approx K_d \frac{de(t)}{dt}} + K_i \int_0^t e\,dt, \tag{24}$$

where $\hat{x}_2$ is the estimate for x_2 obtained from the HGO. The gains are designed in order to match the following equations

$$s^3 + K_d s^2 + K_p s + K_i = 0, \tag{25}$$

$$(s^2 + 2\zeta\omega_n + \omega_n^2)(s+p) = 0, \tag{26}$$

where ω_n, ζ and p are design constants and $K_i := k_i(I_{4\times 4})$, $K_p := k_p(I_{4\times 4})$ and $K_d := k_d(I_{4\times 4})$. Therefore the controller gains are designed in order to approximate the error third order dynamics to a second order system added to a (fast) pole. To this end, the control gains are designed as:

$$k_i := \omega_n^2 p, \tag{27}$$

$$k_p := \omega_n^2 + 2\zeta\omega_n p, \tag{28}$$

$$k_d := p + 2\zeta\omega_n. \tag{29}$$

A. Stability Properties

When uncertainties are presented in the plant parameters and in the HGO estimates, one can write:

$$\ddot{e} + K_d\dot{e} + K_p e + K_i \int_0^t e\,dt = \xi(t), \tag{30}$$

where

$$\begin{aligned} \xi(t) \;&:=\; -D^{-1}(y)(C_n(y,\hat{x}_2) - C(y,x_2))x_2 - \\ &-\; D^{-1}(y)\left[(g_n(y) - g(y)) - C_n(y,\hat{x}_2)\tilde{x}_2)\right] - K_d\tilde{x}_2. \end{aligned} \tag{31}$$

Note that, in the ideal case when the nominal matrices C_n and g_n match the real values and $\hat{x}_2 = x_2$, the following closed-loop equation holds

$$\dddot{e} + K_d\ddot{e} + K_p\dot{e} + K_i e = 0, \tag{32}$$

which assures that $|e(t)| \to 0$ as $t \to \infty$ when $s^3 + K_d s^2 + K_p s + K_i = 0$ has strictly stable roots.

For the general case, when uncertainties are presented in the plant parameters and in the HGO estimates, the tracking error converges (locally) to a residual set of order $\mathcal{O}(\bar{\mu})$, where $\bar{\mu}$ is the small parameter in the time varying HGO parameter $\mu(t)$. In what follows, the stability analysis is carried out for $k_i = 0$ for simplicity. However, the case $k_i \neq 0$ can be treated in a similar fashion.

First, for $k_i = 0$, one has that the closed loop error dynamics becomes $\ddot{e} + K_d\dot{e} + K_p e = \xi(t)$ which can be made ISS w.r.t. ξ by appropriate values of K_p, K_d so that $s^2 + K_d s + K_p$ is a Hurwitz polynomial. Second, by considering the plant state satisfies $\|x(t)\| < M$, $\forall t < t^*$ and some $t^* > t_\mu$, then by applying Lemma 1, the disturbance term norm $\|\xi\|$ is bounded by a constant of order $\mathcal{O}(\bar{\mu})$, *modulo* an exponentially decaying term depending on the HGO initial condition. Since the tracking error dynamics is ISS w.r.t. ξ, then one can conclude that $e(t)$ ultimately converges to a residual set of order $\mathcal{O}(\bar{\mu})$. This is a local convergence property.

On the other hand, when the OFSM control scheme developed in [11] is considered, global/semi-global practical stability results can be guaranteed, even in the presence of those uncertainties. This was left for a future work.

VI. Numerical Simulations

The plant initial conditions are: $y(0) = x_1(0) = \begin{bmatrix} 0.0216 & 0.5675 & -0.13 & -0.39 \end{bmatrix}^T$ and $x_2(0) = \begin{bmatrix} 0 & 0 & 0 & 0 \end{bmatrix}^T$. The PID control gains were obtained by considering $\omega_n = 16\pi$, $\zeta = 0.9$, $p = 2\omega_n$. The time varying HGO gain was implemented as in (21) with $\alpha = 10^{-5}$, $\beta = 1$ and $\hat{x}_1(0) = \hat{x}_2(0) = \begin{bmatrix} 0 & 0 & 0 & 0 \end{bmatrix}^T$.

In the present case, random parametric errors in plant values from [16], such as center of gravity, inertia matrix and link length do not differ by more than 10% from the real ones. A white gaussian noise has also been added to the system output. That helps to illustrate an HGO variable gain application mitigating noise influence.

Simulation results from HGO design with static gain are shown in Figs. 1 to 8. The parameters used are $l_1 = 2$, $l_2 = 6$ and $\mu = \bar{\mu} = 0.001$.

In Fig. 1 to Fig. 4, the desired, estimated and true state trajectory are depicted. It can be seen that the estimation convergences to a small residual set. Peaking phenomenon in position estimation is due to an initial estimation error.

The corresponding hip, thigh, knee and ankle velocities are illustrated in Fig. 5 to Fig. 8. As knee and ankle joints trajectories have faster frequency components, higher gains in control would be needed to reduce velocity tracking RMSE (Root-mean-square-error).

When implementing the HGO, it is important to take in consideration the peaking phenomenon occurring due to its inner characteristics. In order to avoid that, both velocity and control signals are implemented with saturation as depicted in Fig. 8 and Fig. 10.

It can be seen that the HGO with static gain and PID control approach were suitable for the task. Simulations were also conducted using HGO with variable gain to evaluate its performance in the presence of noise and parametric uncertainties. Fig. 9 to Fig. 12 show how changes in μ affect the tradeoff between tracking error and noise energy in control signal.

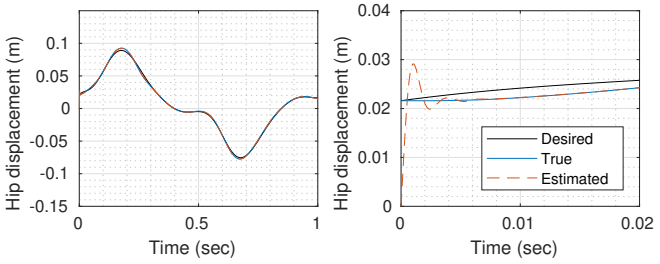

Fig. 1. Simulation results from a desired hip movement, the controlled plant state and the estimated state. The right plot shows the signal in the first 20ms of simulation

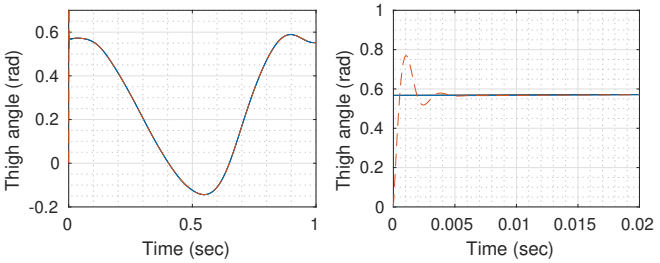

Fig. 2. Simulation results from a desired thigh movement, the controlled plant state and the estimated state from the HGO. The right plot shows the signal in the first 20ms of simulation

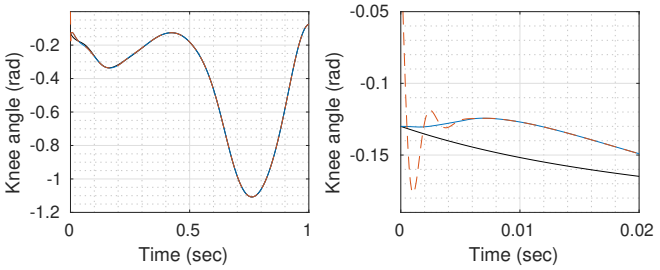

Fig. 3. Simulation results from a desired knee movement, the controlled plant state and the estimated state. The right plot shows the signal in the first 20ms of simulation

A variable HGO gain adaptation is depicted in Fig. 9. In Figs. 11 and Fig. 10 the same legend pattern in applied as in Fig. 9, therefore blue, yellow and red represent μ_1, μ_2 and $\mu_{var}(t)$ respectively.

By applying μ_2, an apparent degradation in the closed-loop tracking error transient is shown in Table I and Fig. 12. On the other hand, the noise amplitude in the control signal is acceptable as can be observed in Fig. 10 with the corresponding measurement of the noise amplitude illustrated in Fig. 11. The noise amplitude was obtained by filtering the control input u with a high-pass filter.

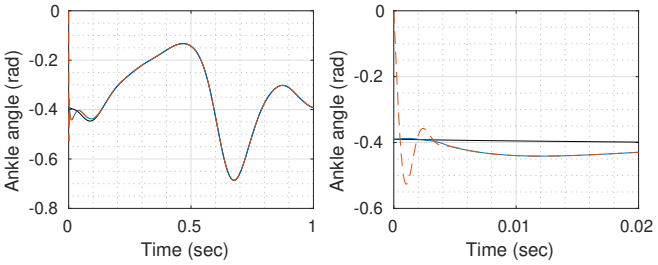

Fig. 4. Simulation results from a desired ankle movement, the controlled plant state and the estimated state. The right plot shows the signal in the first 20ms of simulation

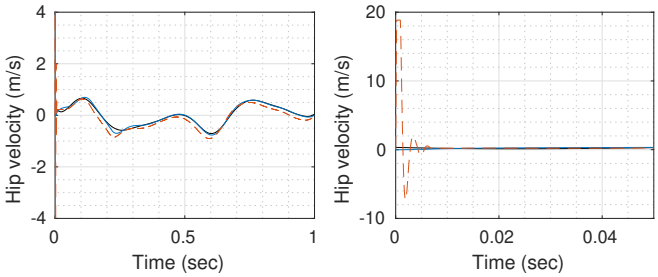

Fig. 5. Simulation results from a desired hip velocity, the controlled plant state and the estimated state. The right plot shows the signals behaviors until the first 50ms of simulation.

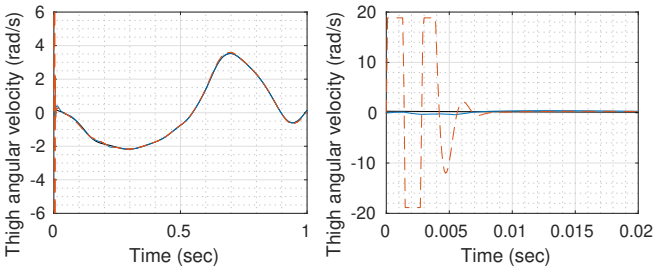

Fig. 6. Simulation results from a desired thigh velocity, the controlled plant state and the estimated state. The right plot shows the signal in the first 20ms of simulation.

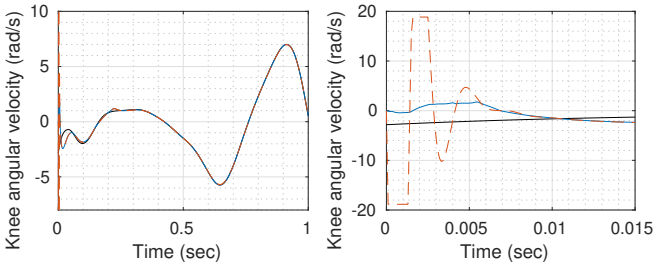

Fig. 7. Simulation results from a desired knee velocity, the controlled plant state and the estimated state. The right plot shows the signal in the first 15ms of simulation.

By reducing μ to the constant small value $\mu_{var}(t) = 0.0004$, the tracking error transient is improved in exchange of an increase on the control signal noise, see Fig.11, FIg. 12 and Table I.

On the other hand, when the time-varying $\mu_{var}(t)$ is implemented starting with the same large value for $\mu_{var}(0) =$

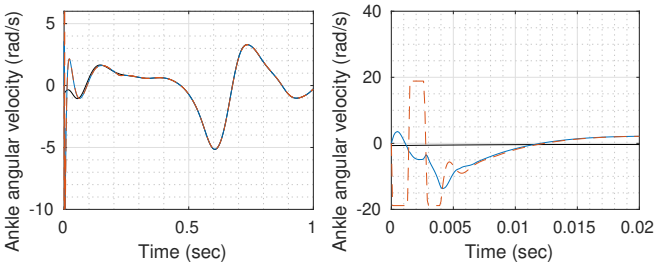

Fig. 8. Simulation results from a desired ankle velocity, the controlled plant state and the estimated state. The right plot shows the signal in the first 20ms of simulation.

TABLE I

RMSE FOR HGO STATES AND THE DESIRED TRAJECTORY IN EACH JOINT OF A PROSTHETIC LEG ACCORDING TO THE OBSERVER GAIN μ

μ	x_1 (m)	x_2 (rad)	x_3 (rad)	x_4 (rad)	$\dot{x}_1$ (m/s)	$\dot{x}_2$ (rad/s)	$\dot{x}_3$ (rad/s)	$\dot{x}_4$ (rad/s)
0.4e-3	0.0004	0.0002	0.0009	0.0004	0.0159	0.0117	0.0959	0.0492
1.9e-3	0.0035	0.0013	0.0033	0.0062	0.1120	0.0587	0.2405	0.6836
Variable	0.0008	0.0004	0.0025	0.0059	0.0257	0.0375	0.2268	0.6640

0.0019, the tracking error transient is improved without reducing μ to a prohibitive value which can cause a large noise in the control signal.

The time evolution of $\mu_{var}(t)$ is shown in Fig.9, from which one can verify that μ reaches a value of $\mu_{var}(t) = 0.001$ depending on the noise power applied to the system. This value is not known *a priori*. It is clear that care must be taken while reducing $\bar{\mu}$, since there exists a trade off between noise reduction and tracking accuracy.

VII. CONCLUSIONS AND FUTURE WORK

In this paper we considered the state estimation problem of a robot/prosthesis control system with vertical hip displacement, thigh, knee and ankle joints. It was verified that it is possible to apply HGO with dynamic gain in order to reduce the amount of noise in the control signal while assuring an reasonable output tracking error transient. Moreover, when a norm observer is available, domination techniques can be used to design the HGO dynamic gain to obtain global/semi-global practical tracking, via sliding mode control. An illustrative academic simulation example was presented.

Future possible topics of research are: (i) consider the full robot/prosthesis model including the ground reaction forces estimation; (ii) replace the conventional PID controller by a smooth version of the output feedback sliding mode controller previous developed in [11] in order to increase the robustness of the closed loop system w.r.t. parameter uncertainties while assuring global/semi-global stability properties and (iii) perform experimental results.

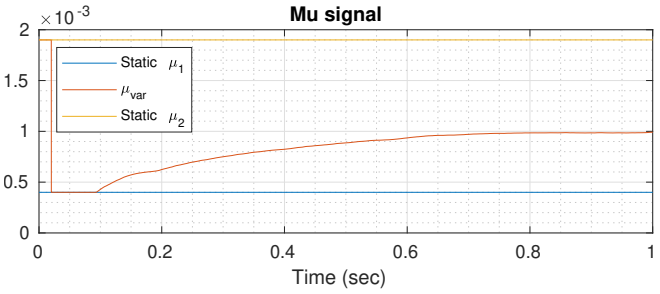

Fig. 9. Simulation results showing the adaptation from a variable μ converging to 0.001.

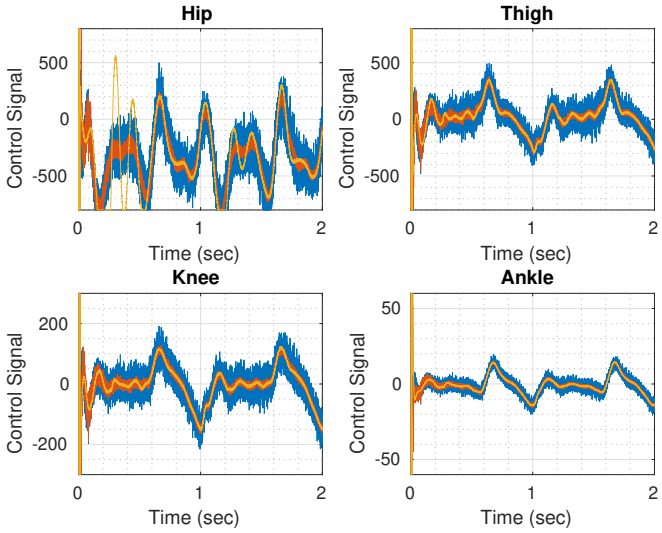

Fig. 10. This graphic shows the difference between gain values and its filtering capacity. The control signal in blue represents the static gain $\mu = 0.0004$, which does not filter the noise as much as $\mu_{var}(t)$ in red or $\mu = 0.0019$ in yellow.

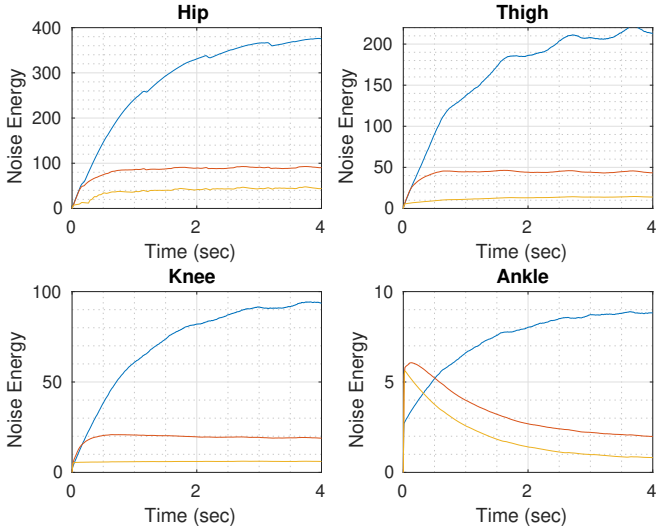

Fig. 11. $\mu_{var}(t)$ in red is able to filter noise as good as $\mu = 0.0019$ in yellow.

REFERENCES

[1] G. M. Sup F, Bohara A, "Design and control of a powered transfemoral prosthesis," *The International journal of robotics research*, vol. 27, no. 2, pp. 263–73, 2008.

[2] B. S, "Actuated leg prosthesis for above knee amputees," Patent US7 314 490B2, 2002.

[3] S. A. Fakoorian and D. Simon, "Ground reaction force estimation in prosthetic legs with an extended kalman filter," *Systems Conference (SysCon), 2016 Annual IEEE*, pp. 1–6, 2016.

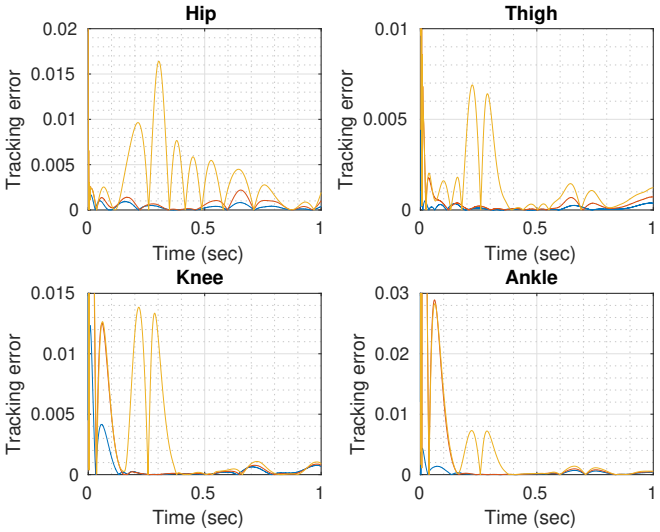

Fig. 12. Using $\mu_{var}(t)$, in red, the system is able to track the trajectory as good as when $\mu = 0.0004$ in blue. For quantitative values, Table I shows tracking RMSE.

[4] J. H. Ahrens and H. K. Khalil, "Closed-loop behavior of a class of nonlinear systems under EKF-based control," *IEEE Trans. Aut. Contr.*, vol. 52, no. 3, pp. 536–540, 2007.

[5] J. H. Ahrens and K. H., "High-gain observers in the presence of measurement noise: A switched-gain approach," *Automatica*, vol. 45, no. 4, 2009.

[6] S. Oh and H. K. Khalil, "Nonlinear output-feedback tracking using high-gain observer and variable structure control," *Automatica*, vol. 33, no. 10, pp. 1845–1856, 1997.

[7] L. Praly, "Asymptotic stabilization via output feedback for lower triangular systems with output dependent incremental rate," in *Proc. IEEE Conf. on Decision and Control*, Orlando, Florida USA, 2001, pp. 3808–3813.

[8] P. Krishnamurthy, F. Khorrami, and Z. P. Jiang, "Global output feedback tracking for nonlinear systems in generalized output-feedback canonical form," *IEEE Trans. Aut. Contr.*, vol. 47, no. 5, pp. 814–819, 2002.

[9] P. Krishnamurthy, F. Khorrami, and R. S. Chandra, "Global high-gain-based observer and backstepping controller for generalized output-feedback canonical form," *IEEE Trans. Aut. Contr.*, vol. 48, no. 12, pp. 2277–2284, 2003.

[10] H. Lei and W. Lin, "Universal output feedback control of nonlinear systems with unknown growth rate," in *Preprints of the 16th IFAC World Congress*, Prague, Czech Republic, July 2005.

[11] A. J. Peixoto, T. R. Oliveira, and L. Hsu, "Global tracking sliding mode control for a class of nonlinear systems via variable gain observer," *International Journal of Robust and Nonlinear Control*, pp. 177–196, 2011.

[12] A. J. Peixoto, L. Hsu, R. R. Costa, and F. Lizarralde, "Global tracking sliding mode control for uncertain nonlinear systems based on variable high gain observer," in *Proc. IEEE Conf. on Decision and Control*, New Orleans, LA, USA, 2007, pp. 2041–2046.

[13] V. Andrieu, L. Praly, and A. Astolfi, "Asymptotic tracking of a state trajectory by output-feedback for a class of non linear systems," in *CDC*, New Orleans, LA, USA, 2007, pp. 5228–5233.

[14] G. Kaliora, A. Astolfi, and L. Praly, "Norm estimators and global output feedback stabilization of nonlinear systems with ISS inverse dynamics," *IEEE Trans. Aut. Contr.*, vol. 51, no. 3, pp. 493–498, 2006.

[15] V. Andrieu, L. Praly, and A. Astolfi, "High gain observers with updated gain and homogeneous correction terms," *Automatica*, vol. 45, no. 2, pp. 422–428, 2009.

[16] H. Richter, D. Simon, W. A. Smith, and S. Samorezov, "Dynamic modeling, parameter estimation and control of a leg prosthesis test robot," *Applied Mathematical Modelling*, vol. 39, no. 2, pp. 559–573, 2015.

[17] M. H. Schwartz, A. Rozumalski, and J. P. Trost, "The effect of walking speed on the gait of typically developing children," *Journal of Biomechanics*, vol. 41, no. 8, pp. 1639 – 1650, 2008. [Online]. Available: http://www.sciencedirect.com/science/article/pii/S0021929008001450

[18] P. Ioannou and J. Sun, *Robust Adaptive Control*. Prentice-Hall, 1996.

[19] H. K. Khalil, *Nonlinear Systems*, 3rd ed. Prentice Hall, 2002.

[20] E. D. Sontag and Y. Wang, "On characterizations of the input-to-state stability property," *Systems & Contr. Letters*, vol. 24, pp. 351–359, 1995.

[21] J. Lee, R. Mukherjee, and H. K. Khalil, "Output feedback stabilization of inverted pendulum on a cart in the presence of uncertainties," *Automatica*, vol. 54, pp. 146–157, 2015.

[22] H. K. Khalil, "High-gain observers in nonlinear feedback control," *2008 International Conference on Control, Automation and Systems*, pp. xlvii – lvii, 2008.